



**HAL**  
open science

# pH-Controlled One Pot Syntheses of Giant Mo<sub>2</sub>O<sub>2</sub>S<sub>2</sub>-Containing Seleno-Tungstate Architectures

Mhamad Aly Moussawi, Sébastien Floquet, Pavel Abramov, Cristian Vicent, Mohamed Haouas, Emmanuel Cadot

► **To cite this version:**

Mhamad Aly Moussawi, Sébastien Floquet, Pavel Abramov, Cristian Vicent, Mohamed Haouas, et al.. pH-Controlled One Pot Syntheses of Giant Mo<sub>2</sub>O<sub>2</sub>S<sub>2</sub>-Containing Seleno-Tungstate Architectures. Inorganic Chemistry, 2018, 57 (1), pp.56-63. 10.1021/acs.inorgchem.7b01644 . hal-02335584

**HAL Id: hal-02335584**

**<https://hal.science/hal-02335584>**

Submitted on 17 Jan 2021

**HAL** is a multi-disciplinary open access archive for the deposit and dissemination of scientific research documents, whether they are published or not. The documents may come from teaching and research institutions in France or abroad, or from public or private research centers.

L'archive ouverte pluridisciplinaire **HAL**, est destinée au dépôt et à la diffusion de documents scientifiques de niveau recherche, publiés ou non, émanant des établissements d'enseignement et de recherche français ou étrangers, des laboratoires publics ou privés.

# pH-controlled one pot syntheses of giant Mo<sub>2</sub>O<sub>2</sub>S<sub>2</sub>-containing selenotungstate architectures

Mhamad Aly Moussawi,<sup>1</sup> Sébastien Floquet,<sup>\*1</sup> Pavel A. Abramov,<sup>\*2,3</sup> Cristian Vicent,<sup>4</sup> Mohamed Haouas,<sup>1</sup> and Emmanuel Cadot.<sup>1</sup>

<sup>1</sup> Institut Lavoisier de Versailles, UMR CNRS 8180, UVSQ, University Paris-Saclay, 45 avenue des Etats-Unis, 78035 Versailles, France.

<sup>2</sup> Nikolaev Institute of Inorganic Chemistry SB RAS, Novosibirsk, Russia, 630090

<sup>3</sup> Novosibirsk State University, Novosibirsk, Russia, 630090

<sup>4</sup> Serveis Centrals d'Instrumentació Científica, Universitat Jaume I, Av. Sos Baynat s/n, 12071 Castelló, Spain

KEYWORDS. Molybdenum, oxo-sulfido binuclear cluster, selenium, polyoxometalate, polyoxotungstate.

Supporting Information Placeholder

**ABSTRACT:** Self-assembly reactions between Na<sub>2</sub>WO<sub>4</sub>, SeO<sub>2</sub>/SeO<sub>3</sub><sup>2-</sup> and [Mo<sub>2</sub>O<sub>2</sub>(μ-S)<sub>2</sub>(H<sub>2</sub>O)<sub>6</sub>]<sup>2+</sup> give, depending on the pH value, two new large polyoxometalate complexes, *i.e.* [(γ-Se<sub>2</sub>W<sub>14</sub>O<sub>52</sub>)<sub>3</sub>(Mo<sub>2</sub>O<sub>2</sub>(μ-S)<sub>2</sub>(H<sub>2</sub>O)<sub>6</sub>)<sub>6</sub>]<sup>24+</sup> (**1**) isolated at pH 3.5 and [(γ-Se<sub>2</sub>W<sub>14</sub>O<sub>52</sub>)<sub>4</sub>(WO<sub>3</sub>(H<sub>2</sub>O))<sub>8</sub>(W<sub>2</sub>O<sub>5</sub>)<sub>2</sub>(W<sub>4</sub>O<sub>12</sub>)<sub>2</sub>(Mo<sub>2</sub>O<sub>2</sub>(μ-S)<sub>2</sub>(H<sub>2</sub>O)<sub>2</sub>)<sub>4</sub>(Mo<sub>2</sub>O<sub>2</sub>(μ-S)<sub>2</sub>(SeO<sub>3</sub>)<sub>4</sub>)<sub>3</sub>]<sup>36-</sup> (**2**) isolated at pH 2. The two compounds were characterized in the solid state by single crystal X-Ray diffraction, EDX, elemental analysis, TGA and FT-IR and in solution by ESI-MS.

## Introduction

Owing to their structural versatility and potential applications in numerous fields such as catalysis,<sup>1</sup> electrocatalysis,<sup>2</sup> medicine,<sup>3</sup> magnetism,<sup>4</sup> materials sciences, and nanotechnology,<sup>5-6</sup> the number of publications concerning polyoxometalates (POMs) exploded over the last decade. This increased interest largely arises from the suitability of pre-formed lacunary POM clusters in which vacancies in the cluster shell can be occupied by additional metal ions or may support the formation of larger metal moieties. Nevertheless, chemists remain fascinated by the rational design and synthesis of gigantic POMs from a fundamental point of view or for applications in various domains. In the field of polyoxomolybdates, and almost two decades ago, Müller *et al.* reported the discovery of a fullerene-like, all-inorganic hollow spheres containing 132 molybdenum centers known as Keplerates.<sup>7</sup> Since their discovery, these compounds have been considerably enriched by numerous groups with a large panel of applications, especially for catalysis in confined spaces. This family of polyoxomolybdates was also complemented by other giant POMs namely the "big wheels" {Mo-154}, {Mo-176} and {Mo-248}, and the "blue lemon" {Mo-368}, which expanded the frontiers of inorganic chemistry to the mesoscopic world.<sup>7-8</sup> In contrast, the synthesis of polyoxotungstate clusters with high nuclearity remains more challenging and limited despite wonderful examples published in recent years. To date, the use of extra linking heteroatoms is required to generate large architectures where the chemists have to choose wisely both the linkers and the building units that will serve to construct such spectacular supramolecular

entities. As building blocks, the heteropolyoxotungstates are based on the assembly of W<sup>VI</sup>O<sub>6</sub> octahedra around heteroanions, which can be for example PO<sub>4</sub><sup>3-</sup>, AsO<sub>4</sub><sup>3-</sup>, SiO<sub>4</sub><sup>4-</sup>, GeO<sub>4</sub><sup>4-</sup>, AsO<sub>3</sub><sup>3-</sup>, SbO<sub>3</sub><sup>3-</sup> or IO<sub>6</sub><sup>5-</sup>. A controlled hydrolysis of the latter provides a large panel of vacant reactive heteropolyoxotungstates, viewed as inorganic ligands. The choice of the heteroelement is determinant since it can seriously affect the final architectures and their physical properties by controlling the range and the connectivity of the building blocks. As linkers, 3d or 4f metals can be chosen, as well as preformed coordination complexes or clusters. In Versailles, our group's main focus is on the use of preformed sulfurated cationic clusters such as [Mo<sup>V</sup><sub>2</sub>O<sub>2</sub>S<sub>2</sub>(H<sub>2</sub>O)<sub>2</sub>]<sup>2+</sup>. While the self-condensation of the aqua complexes [Mo<sub>2</sub>O<sub>2</sub>S<sub>2</sub>(H<sub>2</sub>O)<sub>6</sub>]<sup>2+</sup> produces versatile inorganic macrocyclic structures featuring adjustable host-guest properties,<sup>9</sup> the same [Mo<sub>2</sub>O<sub>2</sub>S<sub>2</sub>(H<sub>2</sub>O)<sub>6</sub>]<sup>2+</sup> moiety proved to be an efficient ditopic unit for reaction with highly negatively-charged polyoxotungstates. The coordination requirements of the {Mo<sub>2</sub>O<sub>2</sub>S<sub>2</sub>}<sup>2+</sup> core are mainly restricted to two equatorial and one axial sites of the two equivalent Mo atoms and the predisposition of the coordinating groups in a predictable self-assembly processes. Controlling the formation of the [Mo<sub>2</sub>O<sub>2</sub>S<sub>2</sub>(H<sub>2</sub>O)<sub>6</sub>]<sup>2+</sup> cation by choosing an appropriate precursor allows adapting the synthetic conditions to the stability and coordination requirements of the vacant heteropolyoxotungstate. A series of polyoxothiometalate compounds has been obtained by controlled addition of the {Mo<sub>2</sub>O<sub>2</sub>S<sub>2</sub>}<sup>2+</sup> unit on preformed mono-, di-, tri-, tetra- and super-lacunary polyoxotungstates. During the last fifteen years it has been combined with almost all common vacant polyoxotungstates such as {XW<sub>9</sub>} (X = P, Si, Sb, As), {XW<sub>10</sub>} (X = Si, P), {XW<sub>11</sub>} (X = B, Si, P), {P<sub>2</sub>W<sub>15</sub>}, {P<sub>2</sub>W<sub>17</sub>}, or {P<sub>8</sub>W<sub>48</sub>} to produce a large panel of nano-sized architectures exhibiting remarkable flexibility in solution.<sup>10</sup> Among the most interesting systems so far are those obtained with {AsW<sub>9</sub>}, probably due to the lone pair steric effect of the As<sup>III</sup> center.<sup>11</sup> For these systems, depending on the experimental conditions and especially the nature of counter cations and the concentration, different assemblies with the same stoichiometry between the POM and the linkers were obtained, *i.e.*, sandwich, tetrahedral, or hexameric arrangements. By the same manner, combination of [Mo<sup>V</sup><sub>2</sub>O<sub>2</sub>S<sub>2</sub>(H<sub>2</sub>O)<sub>6</sub>]<sup>2+</sup> with ammonium heptamolybdate or sodium molybdate in one-pot syntheses led to a family of compounds

varying from a square  $\{\text{Mo}_{40}\}^{12}$  to a discotic compound  $\{\text{Mo}_{63}\}^{13}$  to a cube  $\{\text{Mo}_{84}\}^{14}$  or to some Keplerates  $\{\text{Mo}_{132}\}^{13-14}$ . Once again, the experimental conditions play a crucial role for the selective synthesis in such systems where the nature of the counter-cations, the molar ratio of the reactants, the concentrations and the pH must be carefully controlled.

In this context, we were prompted to investigate the formation of new original architectures associating  $[\text{Mo}_2\text{O}_2\text{S}_2(\text{H}_2\text{O})_6]^{2+}$ , tungstate and selenite anion  $\text{SeO}_3^{2-}$  using one-pot procedures. The  $\text{Se}^{\text{IV}}$  atom of this anion contains a lone-pair which can be exploited since it can generate lacunary polyoxotungstates without the need to hydrolyze the pre-existing parent clusters. This advantage allows the preparation of unique, often high nuclearity, POM architectures when they are associated to transition metals. Indeed, the use of the selenite  $\text{SeO}_3^{2-}$  anion prevents the closure of the cluster assemblies to the Keggin or the Dawson-type clusters, and instead gives rise to open lacunary units  $\{\text{SeW}_9\}$  or  $\{\text{Se}_2\text{W}_{12}\}$  and their derivatives. The former is usually obtained at pH greater than 4 while the latter is more easily obtained in more acidic medium. In the last years, very spectacular supramolecular assemblies were published by different groups. By one pot-synthesis, various architectures were recently reported such as  $[\text{H}_2\text{SeW}_{18}\text{O}_{60}]^{6-,15}$ ,  $[\text{Mn}_4\text{Se}_6\text{W}_{24}\text{O}_{94}\text{Cl}(\text{H}_2\text{O})_6]^{13-,16}$ ,  $[(\text{Se}_2\text{W}_{12}\text{O}_{46}(\text{WO}(\text{H}_2\text{O}))_3)]^{24-,16}$ ,  $[\text{H}_{12}\text{Pd}_{10}\text{Se}_{10}\text{W}_{52}\text{O}_{206}]^{28-}$  and  $[\text{H}_{14}\text{Pd}_{10}\text{Se}_{10}\text{W}_{52}\text{O}_{206}]^{26-,17}$ ,  $[\text{H}_2\text{W}_{43}\text{Se}_3\text{O}_{148}]^{24-}$ ,  $[\text{H}_4\text{W}_{77}\text{Se}_5\text{O}_{265}]^{44-}$  and  $[\text{H}_6\text{W}_{63}\text{Se}_6\text{O}_{221}]^{34-,18}$ ,  $[\text{H}_{19}\text{Co}_{2.5}(\text{W}_{3.5}\text{O}_{14})(\text{SeW}_9\text{O}_{33})(\text{Se}_2\text{W}_{30}\text{O}_{107})]^{17-}$ ,  $[\text{H}_4\text{CoWO}(\text{H}_2\text{O})_3(\text{Se}_2\text{W}_{26}\text{O}_{85})(\text{Se}_3\text{W}_{30}\text{O}_{107})_2]^{40-}$  and  $[\text{H}_{14}\text{Ni}_2\text{W}_2\text{O}_2\text{Cl}(\text{H}_2\text{O})_3(\text{Se}_2\text{W}_{29}\text{O}_{103})(\text{Se}_3\text{W}_{30}\text{O}_{107})_2]^{43-,19}$  and  $[(\text{SeO}_3)\text{W}_{10}\text{O}_{34}]_8\{\text{Ce}_8(\text{H}_2\text{O})_{20}\}(\text{WO}_2)_4(\text{W}_4\text{O}_{12})]^{48-}$  and  $[(\text{SeO}_3)\text{W}_{10}\text{O}_{34}]_8\{\text{Ce}_8(\text{H}_2\text{O})_{20}\}(\text{WO}_2)_4\{\text{W}_4\text{O}_6\}\text{Ce}_4(\text{H}_2\text{O})_{14}(\text{SeO}_3)_4(\text{NO}_3)_2]^{34-,20}$  or  $[(\alpha\text{-SeW}_9\text{O}_{34})\{\text{Zr}(\text{H}_2\text{O})\}\{\text{WO}(\text{H}_2\text{O})\}(\text{WO}_2)(\text{SeO}_3)\{\alpha\text{-SeW}_8\text{O}_{31}\text{Zr}(\text{H}_2\text{O})\}]_2^{12-}$ ,  $[(\text{Se}_2\text{W}_{18}\text{O}_{60})_2(\mu_2\text{-O})_4]^{16-}$ ,  $[\text{Se}_2\text{W}_{18}\text{O}_{62}(\text{H}_2\text{O})_2]^{8-}$ ,  $[(\alpha\text{-SeW}_9\text{O}_{33})_2\{\text{Ce}_2(\text{CH}_3\text{COO})(\text{H}_2\text{O})_3\text{W}_3\text{O}_6\}(\alpha\text{-Se}_2\text{W}_{14}\text{O}_{52})]^{17-}$  and  $[(\alpha\text{-SeW}_9\text{O}_{33})_2\{\text{Ce}_2(\text{H}_2\text{O})_4\text{W}_3\text{O}_6\}\{\alpha\text{-Se}_2\text{W}_{14}\text{O}_{51}(\text{OH})\}]^{15-,21}$ . For all of them, the reactions were performed in aqueous medium under controlled pH, which appears to be a key parameter for the formation of these systems and especially their building blocks. Based on a similar approach, we investigate the ternary system  $\text{WO}_4^{2-}/\text{SeO}_3^{2-}/\{\text{Mo}_2\text{O}_2\text{S}_2\}^{2+}$  at different pH values. At pH ca 3.5 a triangle-like hybrid complex **1** is isolated while at lower pH it recombines to a giant complex **2**. Their syntheses and characterization are described in this study.

## Experimental part

### Physical methods

**Fourier Transformed Infrared (FT-IR)** spectra were recorded on a 6700 FT-IR Nicolet spectrophotometer, using diamond ATR technique. The spectra were recorded on non-diluted compounds and ATR correction was applied. **Elemental analyses** were carried out by the analytical service of the CNRS at Gif sur Yvette, France (C, H, N, S) or by ICP-AES at NIIC, Novosibirsk, Russia (Na, K, S, Se, Mo, W). **Energy-dispersive X-ray spectroscopy (EDX)** measurements were performed on a JEOL JSM 5800LV apparatus. **Water content** was determined by thermal gravimetric (TGA) analysis with a Seiko TG/DTA 320 thermogravimetric balance ( $5^\circ\text{C min}^{-1}$ , under  $\text{N}_2$ ). **NMR studies** in  $\text{D}_2\text{O}$  solution at room temperature were carried out on a Bruker Avance 400 spectrometer operating at 76.41 MHz for  $^{77}\text{Se}$  nucleus and 16.67 MHz for  $^{183}\text{W}$  nucleus. Typical spectra were acquired with 8k to 16k and 32k number of scans for  $^{77}\text{Se}$  and  $^{183}\text{W}$  requiring ca. 18-20 h and 18 h measurement times, respectively.  $^{77}\text{Se}$  chemical shift was referenced to external  $\text{Na}_2\text{SeO}_3$  ( $\delta = 1273$  ppm) and then recalculated vs  $\text{SeMe}_2$  ( $\delta = 0$  ppm).<sup>22</sup> The  $^{183}\text{W}$  NMR scale was calibrated relative to the signal of  $\text{D}_2\text{O}/\text{H}_2\text{O}$  solution of  $\text{H}_4\text{SiW}_{12}\text{O}_{40}$  at -103.8 ppm with respect to the saturated  $\text{Na}_2\text{WO}_4$

solution. The  $^{77}\text{Se}$  MAS NMR experiments were performed on a Bruker Avance 500 spectrometer equipped with a 11.7 T wide-bore magnet. The resonance frequency was 95.50 MHz and the experiments were performed with a 3.2 mm MAS probe and a spinning rate of 20 kHz. Hahn echo MAS spectra were recorded with 32K data points and a recycle delay of 61 s.

**Electrospray Ionization Mass Spectrometry.** A Q-TOF premier mass spectrometer with an orthogonal Z-spray electrospray source (Waters, Manchester, U.K.) was used. The temperature of the source block was set to  $100^\circ\text{C}$ , while the desolvation temperature was set to  $200^\circ\text{C}$ . A capillary voltage of 3.3 kV was applied in the negative scan mode, and the cone voltage was set to 10 V to control the extent of fragmentation of the identified species. TOF mass spectra were acquired in the V-mode operating at a resolution of ca. 10000 (FWHM). At this resolution, the isotopic pattern of the large 1 and 2 polyanions could not be resolved; however, an estimation of the molecular weight can be conveniently assessed taking into consideration the spacing between the series of peaks in the ESI mass spectra. Mass calibration from  $m/z$  50 to 3000 was performed with a solution of sodium iodide in a 2-propanol/water (50:50) mixture. Aqueous sample solutions were infused via a syringe pump directly connected to the ESI source at a flow rate of  $10 \mu\text{L min}^{-1}$ .

**X-Ray diffraction on single crystals.** Crystallographic data and refinement details are given in Table 1. Because crystals of **Na-1** and **Na-2** quickly lose water of crystallization and become amorphous in air, mineral oil was used to protect the crystals from decay. The diffraction data were collected on a Bruker Apex Duo diffractometer with  $\text{MoK}\alpha$  radiation ( $\lambda = 0.71073 \text{ \AA}$ ) by doing  $\varphi$  and  $\omega$  scans of narrow ( $0.5^\circ$ ) frames at 150 K. An empirical absorption correction was applied using the SADABS program<sup>23</sup>. Both structures were solved by direct methods and refined by full-matrix least-squares treatment against  $|F|^2$  in anisotropic approximation with SHELX 2014/7 set<sup>24</sup> using ShelXle program.<sup>25</sup>

In the case of complex **Na-1** we could find optimal crystal size and minimize artifact electronic density down to 2.79 e. The resulting refinement allowed localizing 13 sodium and one potassium cations, whereas 22  $\text{Na}^+$  and 2  $\text{K}^+$  were found by elemental analysis and EDX measurements to balance the charge of  $[(\text{Se}_2\text{W}_{14}\text{O}_{52})_3(\text{Mo}_2\text{O}_2(\mu\text{-S})_2(\text{H}_2\text{O})_2)_6]^{24-}$ . These discrepancies are typical of large, highly charged and highly solvated polyoxometalates for which alkali atoms are probably disordered with the 75 water molecules in several positions. The anion  $\{\gamma\text{-}(\text{Se}_2\text{W}_{14}\text{O}_{52})_3(\text{Mo}_2\text{O}_2(\mu\text{-S})_2(\text{H}_2\text{O})_2)_6\}^{24-}$  has six  $\{\text{Mo}_2\text{O}_2(\mu\text{-S})_2(\text{H}_2\text{O})_2\}^{2+}$  bridges connecting three  $\{\gamma\text{-}\text{Se}_2\text{W}_{14}\text{O}_{52}\}$  units. Four of these linkers are disordered over two positions. The disorder can be modeled by rotation of each *cis*- $\{\text{Mo}_2\text{O}_2(\mu\text{-S})_2(\text{H}_2\text{O})_2\}^{2+}$  unit by  $180^\circ$  while keeping equal the positions of S, O and  $\text{H}_2\text{O}$ . A related case of such disorder was reported by Cadot et al. in  $[(\text{PW}_{11}\text{O}_{39})_2(\text{Mo}_4\text{S}_4\text{O}_4(\text{OH})_2)]^{10-,26}$ .

In **Na-2** the highest difference peak of 3.96 e is a truncation error arising from Fourier series, and it is typical for the structures with a large number of heavy atoms, and in particular for tungsten containing polyoxometalates. The appearance of such artifacts is due to high X-ray absorption of heavy metals. Smaller crystals of complex **Na-2** diffract poorly. Four outer  $\{\text{Mo}_2\text{O}_2(\mu_2\text{-S})_2(\text{H}_2\text{O})_2\}^{2+}$  units have disordered Mo atoms over two close positions with 0.1/0.9 occupancies. This disorder does not influence the geometry of ligand arrangement because the positions of oxygen atoms of  $\text{Mo}=\text{O}$  and  $\text{Mo}-\text{H}_2\text{O}$  are overlapped. This situation can be viewed as a rotation of the  $\{\text{Mo}_2\text{O}_2(\mu_2\text{-S})_2(\text{H}_2\text{O})_2\}^{2+}$

**Table 1. Crystallographic data for compounds Na-1 and Na-2. Experiments were carried out at 150 K with Mo K $\alpha$  radiation using a Bruker Apex Duo. Absorption was corrected for by multi-scan methods, *SADABS* (Bruker-AXS, 2004).**

	Na-1	Na-2
Chemical formula	KMo <sub>12</sub> Na <sub>13</sub> O <sub>242</sub> S <sub>12</sub> Se <sub>6</sub> W <sub>42</sub>	K <sub>0.80</sub> Mo <sub>16</sub> Na <sub>17.20</sub> O <sub>416</sub> S <sub>16</sub> Se <sub>12</sub> W <sub>76</sub>
Mr	13909.43	24050.83
Crystal system, space group	Orthorhombic, <i>Pbcm</i>	Triclinic, <i>P-1</i>
<i>a</i> , <i>b</i> , <i>c</i> (Å)	17.9677 (7), 43.3408 (15), 37.8230 (14)	17.6801 (17), 23.857 (2), 31.133 (3)
$\alpha$ , $\beta$ , $\gamma$ (°)	90, 90, 90	101.709 (2), 90.277 (2), 105.394 (2)
<i>V</i> (Å <sup>3</sup> )	29454.1 (19)	12373 (2)
Z	4	1
$\mu$ (mm <sup>-1</sup> )	17.77	19.04
Crystal size (mm)	0.10 × 0.05 × 0.05	0.15 × 0.12 × 0.08
<i>T</i> <sub>min</sub> , <i>T</i> <sub>max</sub>	0.566, 0.743	0.310, 0.745
No. of measured, independent and observed [ <i>I</i> > 2 $\sigma$ ( <i>I</i> )] reflections	171656, 31808, 19109	107431, 50323, 29898
R <sub>int</sub>	0.099	0.045
$\theta$ values (°)	$\theta_{\max} = 27.6$ , $\theta_{\min} = 1.6$	$\theta_{\max} = 26.4$ , $\theta_{\min} = 1.2$
( $\sin \theta/\lambda$ ) <sub>max</sub> (Å <sup>-1</sup> )	0.651	0.625
Range of <i>h</i> , <i>k</i> , <i>l</i>	-23 ≤ <i>h</i> ≤ 23, -56 ≤ <i>k</i> ≤ 50, -49 ≤ <i>l</i> ≤ 40	-22 ≤ <i>h</i> ≤ 22, -28 ≤ <i>k</i> ≤ 29, -38 ≤ <i>l</i> ≤ 38
<i>R</i> [ <i>F</i> <sup>2</sup> > 2 <i>s</i> ( <i>F</i> <sup>2</sup> )], <i>wR</i> ( <i>F</i> <sup>2</sup> ), <i>S</i>	0.078, 0.164, 1.12	0.065, 0.201, 1.05
No. of reflections, parameters, restraints	31808, 1533, 36	50323, 2465, 24
Weighting scheme	$w = 1/[\sigma^2(F_o^2) + (0.0184P)^2 + 2575.1055P]$ where $P = (F_o^2 + 2F_c^2)/3$	$w = 1/[\sigma^2(F_o^2) + (0.0777P)^2 + 778.140P]$ where $P = (F_o^2 + 2F_c^2)/3$
$\Delta\rho_{\max}$ , $\Delta\rho_{\min}$ (e Å <sup>-3</sup> )	2.79, -3.49	3.96, -3.32
Goodness of Fit (GOF)	1.119	1.054

Computer programs: *APEX2* (Bruker-AXS, 2004), *SAINTE* (Bruker-AXS, 2004), *SHELXS2014* (Sheldrick, 2014), *SHELXL2014* (Sheldrick, 2014), *SHELXL* (Sheldrick, 2011), *CIFTAB-2014* (Sheldrick, 2014).

unit by 180°. Furthermore, two {WO(H<sub>2</sub>O)}<sup>4+</sup> fragments (W=O 1.715(2), W-O<sub>H<sub>2</sub>O</sub> 2.341(2) Å) are connected to the four {Se<sub>2</sub>W<sub>14</sub>O<sub>52</sub>} units and they show disorder of W atoms over two close positions with 0.65/0.35 or 0.55/0.45 occupancies, the positions of oxygen atoms also being overlapped. The possible reason of such disorder is the rotation of the {Mo<sub>2</sub>O<sub>2</sub>( $\mu$ -S)<sub>2</sub>(H<sub>2</sub>O)<sub>2</sub>}<sup>2+</sup> units causing water molecules of the {WO(H<sub>2</sub>O)} groups to be directed outside the cavity when the water molecules of the Mo/S cluster units are directed to the inside. The positions of Na<sup>+</sup> and K<sup>+</sup> cations were found according to typical distances and geometry. Similarly to **Na-1**, only 17.2 Na<sup>+</sup> and 0.8 K<sup>+</sup> were localized in the X-Ray structure while the elemental analysis and EDX gives 37 Na<sup>+</sup> and 3 K<sup>+</sup> cations. The missing cations are disordered with the 130 water molecules which solvate the polyanion. Finally, the structure of **Na-2** displays more complicated disorder of all central moieties, which arises from two different orientations of [(Se<sub>2</sub>W<sub>14</sub>O<sub>52</sub>)<sub>4</sub>(WO<sub>3</sub>(H<sub>2</sub>O))<sub>8</sub>(W<sub>2</sub>O<sub>5</sub>)<sub>2</sub>(W<sub>4</sub>O<sub>13</sub>)<sub>2</sub>(Mo<sub>2</sub>O<sub>2</sub>( $\mu$ -S)<sub>2</sub>(H<sub>2</sub>O)<sub>2</sub>)<sub>4</sub>(Mo<sub>2</sub>O<sub>2</sub>( $\mu$ -S)<sub>2</sub>(SeO<sub>3</sub>)<sub>4</sub>)<sub>4</sub>]<sup>40-</sup> anion in the crystal structure depicted on Figure S7 (Supporting Information). The left orientation is dominant and fills 92% of all positions in the crystal. The occupancies of W atoms from right orientation are only 8% that does not allow finding positions of their oxygen ligands. The existence of these orientations is possibly due to the fact of practically identical positions of four { $\gamma$ -Se<sub>2</sub>W<sub>14</sub>O<sub>52</sub>} units, which are the heaviest parts of the anion. Crystallographic data for **Na-1** and **Na-2** are summarized in Table 1 whereas Figures 1 to 4 give some pictures of the polyoxometalate moieties. Further details may be obtained from the CCDC. The CCDC numbers are 1559983 for the compound called **Na-1** and 1559984 for the compound called **Na-2**.

## Syntheses

Starting precursor K<sub>2-x</sub>(NMe<sub>4</sub>)<sub>x</sub>[I<sub>2</sub>Mo<sub>10</sub>O<sub>10</sub>S<sub>10</sub>(OH)<sub>10</sub>(H<sub>2</sub>O)<sub>5</sub>]:20H<sub>2</sub>O (*x* = 0-0.5) was prepared according to literature.<sup>27</sup> All other reagents were of commercial quality and used without additional purification.

**Synthesis of Na<sub>22</sub>K<sub>2</sub>[(W<sub>14</sub>Se<sub>2</sub>O<sub>52</sub>)<sub>3</sub>(Mo<sub>2</sub>O<sub>2</sub>( $\mu$ -S)<sub>2</sub>(H<sub>2</sub>O)<sub>2</sub>)<sub>6</sub>]:75H<sub>2</sub>O (**Na-1**).** 5.0 g of Na<sub>2</sub>WO<sub>4</sub>·2H<sub>2</sub>O (15.15 mmol) were dissolved in distilled water (20 mL) and 0.25 g of SeO<sub>2</sub> (2.25 mmol) were then added (pH 8.4). The pH was lowered to 4.7 using 4 M HCl. A milky white precipitate formed locally by addition of HCl re-dissolved rapidly upon stirring. The resulting colorless solution was stirred at room temperature for further 30 min and 1 g of the precursor compound K<sub>2-x</sub>(NMe<sub>4</sub>)<sub>x</sub>[I<sub>2</sub>Mo<sub>10</sub>O<sub>10</sub>S<sub>10</sub>(OH)<sub>10</sub>(H<sub>2</sub>O)<sub>5</sub>]:20H<sub>2</sub>O (0.416 mmol of Mo<sub>10</sub> which give 2.08 mmol of [Mo<sub>2</sub>O<sub>2</sub>S<sub>2</sub>]<sup>2+</sup> clusters) was then added. The yellow solid dissolved within few minutes, whereupon the pH was lowered to 3.5 with 4 M HCl. The resulting clear red solution was stirred at room temperature for 2 h and left to evaporate in an open beaker. Slow evaporation yielded 1.81 g of dark-red crystals which were isolated by filtration and recrystallized in 0.1 M NaCl aqueous solution (60 mL) to give - after 10 days - well-shaped prismatic dark-red crystals of Na<sub>22</sub>K<sub>2</sub>[(W<sub>14</sub>Se<sub>2</sub>O<sub>52</sub>)<sub>3</sub>(Mo<sub>2</sub>O<sub>2</sub>( $\mu$ -S)<sub>2</sub>(H<sub>2</sub>O)<sub>2</sub>)<sub>6</sub>]:75H<sub>2</sub>O, denoted hereafter compound **Na-1**. After recording the X-Ray structure, the crystals were isolated by filtration, washed with cold water, ethanol and ether. Yield 1.1 g, 22%. IR/cm<sup>-1</sup> (see Figure S1, Supporting Information): 1622 (s), 951 (ms), 889 (w), 831 (s), 821 (sh), 758 (vs), 663 (sh), 597 (sh). Elemental analysis calcd (%) for Na<sub>22</sub>K<sub>2</sub>[(W<sub>14</sub>Se<sub>2</sub>O<sub>52</sub>)<sub>3</sub>(Mo<sub>2</sub>O<sub>2</sub>( $\mu$ -S)<sub>2</sub>(H<sub>2</sub>O)<sub>2</sub>)<sub>6</sub>]:75H<sub>2</sub>O (M = 14570.7 g.mol<sup>-1</sup>) H 1.20; K 0.54; Mo 7.90; Na 3.47; S 2.64; Se 3.25; W 52.99. Found (%): H 1.15; K

0.62 ; Mo 8.00 ; Na 3.63 ; S 2.65 ; Se 3.36 ; W 51.95. Absence of C and N which could be due to traces of TMA<sup>+</sup> cations from the precursor. EDX atomic ratios calculated for Na<sub>22</sub>K<sub>2</sub>[( $\gamma$ -W<sub>14</sub>Se<sub>2</sub>O<sub>52</sub>)<sub>3</sub>(Mo<sub>2</sub>O<sub>2</sub>( $\mu$ -S)<sub>2</sub>(H<sub>2</sub>O)<sub>2</sub>)<sub>6</sub>]-75H<sub>2</sub>O (found): Mo/S = 1 (1.10); W/Mo = 3.5 (3.3); W/Se = 7.0 (7.8); Mo/Se = 2 (2.4) W/Na = 1.90 (2.3). TGA: A weight loss of 10.7% between RT and 300 °C corresponds to crystallization and coordinated water molecules (cald: 10.74%).

**Synthesis of Na<sub>37</sub>K<sub>3</sub>[(W<sub>16</sub>Se<sub>2</sub>O<sub>58</sub>(H<sub>2</sub>O)<sub>2</sub>)<sub>4</sub>(W<sub>2</sub>O<sub>5</sub>)<sub>2</sub>(W<sub>4</sub>O<sub>13</sub>)<sub>2</sub>(Mo<sub>2</sub>O<sub>2</sub>( $\mu$ -S)<sub>2</sub>(H<sub>2</sub>O)<sub>2</sub>)<sub>4</sub>(Mo<sub>2</sub>O<sub>2</sub>( $\mu$ -S)<sub>2</sub>(SeO<sub>3</sub>)<sub>4</sub>)]·130H<sub>2</sub>O (Na-2):** 5 g of Na<sub>2</sub>WO<sub>4</sub>·2H<sub>2</sub>O (15.15 mmol) and 0.25 g (2.25 mmol) of SeO<sub>2</sub> were solubilized in water (20 ml, pH = 8.4). The pH was lowered to 4.7 with 4 M HCl (about 5 mL added) and the resulting colorless solution was stirred at room temperature for further 30 min. 0.76 g of K<sub>2-x</sub>(NMe<sub>4</sub>)<sub>x</sub>[I<sub>2</sub>Mo<sub>10</sub>O<sub>10</sub>S<sub>10</sub>(OH)<sub>10</sub>(H<sub>2</sub>O)<sub>5</sub>]-20H<sub>2</sub>O were then added (0.32 mmol of Mo<sub>10</sub> which give 1.58 mmol of [Mo<sub>2</sub>O<sub>2</sub>S<sub>2</sub>]<sup>2+</sup> clusters). The yellow solid dissolved within few minutes, whereupon the pH was lowered to 2.1 with 4 M HCl (the solution turned dark-red at pH below 2.5). The clear dark-red solution was stirred at room temperature for 2 h, and then was kept in air for slow evaporation at room temperature. After one week, dark red single crystals mixed with powder were obtained (1.1 g). The crystals were isolated by filtration on a glass frit n°4 and then recrystallized in water at pH = 2.1 to give dark red single crystals suitable for X-Ray diffraction study after 10 days. Yield 0.53 g, 10 %. Crystals were isolated by filtration and kept in air. IR/cm<sup>-1</sup> (see Figure S2, Supporting Information): 1624 (s), 956 (ms), 889 (m), 831 (s), 750 (vs), 600 (sh), 501 (br., w.). Elemental analysis calcd (%) for Na<sub>37</sub>K<sub>3</sub>[(W<sub>16</sub>Se<sub>2</sub>O<sub>58</sub>(H<sub>2</sub>O)<sub>2</sub>)<sub>4</sub>(W<sub>2</sub>O<sub>5</sub>)<sub>2</sub>(W<sub>4</sub>O<sub>13</sub>)<sub>2</sub>(Mo<sub>2</sub>O<sub>2</sub>( $\mu$ -S)<sub>2</sub>(H<sub>2</sub>O)<sub>2</sub>)<sub>4</sub>(Mo<sub>2</sub>O<sub>2</sub>( $\mu$ -S)<sub>2</sub>(SeO<sub>3</sub>)<sub>4</sub>)]·130H<sub>2</sub>O (M = 25122 g.mol<sup>-1</sup>) H 1.09 ; K 0.47 ; Mo 6.11 ; Na 3.39 ; S 2.04 ; Se 3.77 ; W 55.62. Found (%): H 1.15; K 0.41 ; Mo 5.64 ; Na 3.02 ; S 2.12 ; Se 3.39 ; W 56.28. Absence of C and N which could be due to traces of TMA<sup>+</sup> cations from the precursor. EDX atomic ratios calculated for Na<sub>37</sub>K<sub>3</sub>[(W<sub>16</sub>Se<sub>2</sub>O<sub>58</sub>(H<sub>2</sub>O)<sub>2</sub>)<sub>4</sub>(W<sub>2</sub>O<sub>5</sub>)<sub>2</sub>(W<sub>4</sub>O<sub>13</sub>)<sub>2</sub>(Mo<sub>2</sub>O<sub>2</sub>( $\mu$ -S)<sub>2</sub>(H<sub>2</sub>O)<sub>2</sub>)<sub>4</sub>(Mo<sub>2</sub>O<sub>2</sub>( $\mu$ -S)<sub>2</sub>(SeO<sub>3</sub>)<sub>4</sub>)]·130H<sub>2</sub>O (found): W/Mo = 4.75 (4.53); Mo/S = 1.0 (1.02); W/S = 4.75 (4.60); Mo/Se = 1.33 (1.66), W/Na = 2.05 (2.17), Na/K = 12.33 (12.35). TGA: A weight loss of 9.7% between RT and 300 °C corresponds to crystallization and coordinated water molecules (cald: 9.74%).

## Results and discussion

### Syntheses and structures

By mixing sodium tungstate, selenium dioxide and K<sub>2-x</sub>(NMe<sub>4</sub>)<sub>x</sub>[I<sub>2</sub>Mo<sub>10</sub>O<sub>10</sub>S<sub>10</sub>(OH)<sub>10</sub>(H<sub>2</sub>O)<sub>5</sub>]-20H<sub>2</sub>O in water at pH 3.5, the resulting solution turns red, a color typical of the reaction of nucleophilic [Mo<sub>2</sub>O<sub>2</sub>S<sub>2</sub>]<sup>2+</sup> clusters with vacant polyoxotungstates.<sup>10-11, 28-29</sup> At this pH, the condensation process of [Mo<sub>2</sub>O<sub>2</sub>S<sub>2</sub>]<sup>2+</sup> complexes can also occur to give cyclic assemblies around various ligands<sup>9, 30</sup> and especially around the monotungstate group, which leads to the formation of a very stable yellow-orange compound [Mo<sub>8</sub>O<sub>8</sub>S<sub>8</sub>(OH)<sub>8</sub>(HWO<sub>5</sub>(H<sub>2</sub>O))]·31H<sub>2</sub>O.<sup>31</sup> This species is evidenced by the formation of a yellow precipitate during the synthesis when reactants are introduced in stoichiometric ratios. In order to avoid the formation of the latter, the quantity of the precursor K<sub>2-x</sub>(NMe<sub>4</sub>)<sub>x</sub>[I<sub>2</sub>Mo<sub>10</sub>O<sub>10</sub>S<sub>10</sub>(OH)<sub>10</sub>(H<sub>2</sub>O)<sub>5</sub>]-20H<sub>2</sub>O was reduced until obtaining only a limpid red solution. The quantity of [Mo<sub>2</sub>O<sub>2</sub>S<sub>2</sub>]<sup>2+</sup> is thus introduced below the stoichiometry corresponding to the target compound [( $\gamma$ -Se<sub>2</sub>W<sub>14</sub>O<sub>52</sub>)<sub>3</sub>(Mo<sub>2</sub>O<sub>2</sub>( $\mu$ -S)<sub>2</sub>(H<sub>2</sub>O)<sub>2</sub>)<sub>6</sub>]<sup>24-</sup>, denoted hereafter **1**. After several days the synthesis solution yields dark-red crystals, which are recrystallized from 0.1 M NaCl. Elemental analysis, EDX and TGA measurements lead to the formula

Na<sub>22</sub>K<sub>2</sub>[( $\gamma$ -W<sub>14</sub>Se<sub>2</sub>O<sub>52</sub>)<sub>3</sub>(Mo<sub>2</sub>O<sub>2</sub>( $\mu$ -S)<sub>2</sub>(H<sub>2</sub>O)<sub>2</sub>)<sub>6</sub>]-75H<sub>2</sub>O, denoted hereafter **Na-1**. It crystallizes in the orthorhombic *Pbcm* space group and the molecular structure of **1** is depicted in Figure 1, whereas the crystallographic data are summarized in Table 1.

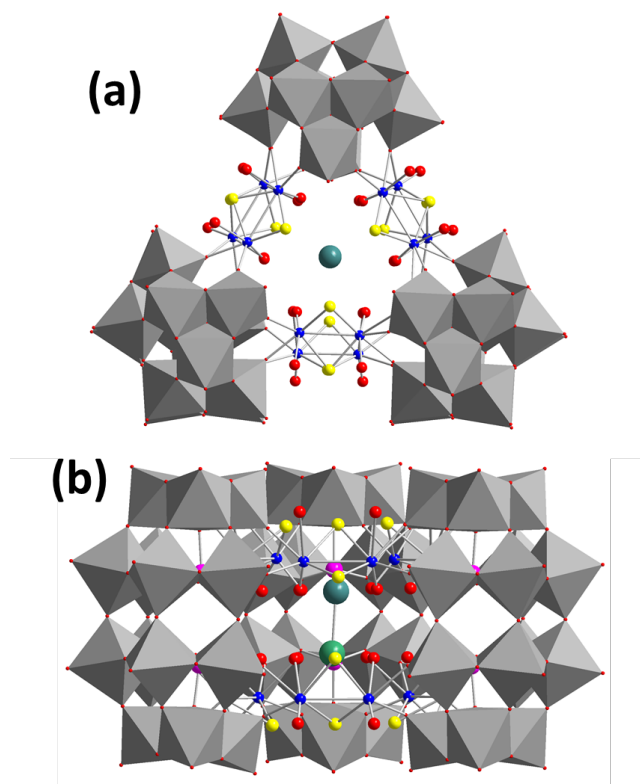


Figure 1. Top (a) and side (b) views of the molecular structure of anion **1**. { $\gamma$ -Se<sub>2</sub>W<sub>14</sub>} units are represented in grey polyhedra while the Se atoms of two central SeO<sub>3</sub><sup>2-</sup> anions are given in pink; [Mo<sub>2</sub>O<sub>2</sub>S<sub>2</sub>(H<sub>2</sub>O)<sub>2</sub>]<sup>2+</sup> linkers are depicted in ball and stick (Mo in blue, S in yellow, O in red); central disordered K<sup>+</sup> cation is also depicted in green.

It consists of triangular {( $\gamma$ -Se<sub>2</sub>W<sub>14</sub>O<sub>52</sub>)<sub>3</sub>(Mo<sub>2</sub>O<sub>2</sub>( $\mu$ -S)<sub>2</sub>(H<sub>2</sub>O)<sub>2</sub>)<sub>6</sub>]<sup>24-</sup> macrocyclic anions, with the ideal *D*<sub>3h</sub> geometry, connected together with sodium cations into two types of puckered layers (Figure S3, SI). The anion has six {Mo<sub>2</sub>O<sub>2</sub>( $\mu$ -S)<sub>2</sub>(H<sub>2</sub>O)<sub>2</sub>]<sup>2+</sup> bridges connecting three tetravacant { $\gamma$ -Se<sub>2</sub>W<sub>14</sub>O<sub>52</sub>} units, which are derivatives of the Dawson-like parent [Se<sub>2</sub>W<sub>18</sub>O<sub>62</sub>]<sup>8-</sup>. These {Se<sub>2</sub>W<sub>14</sub>} units correspond to the gamma isomer and differ from the { $\alpha$ -Se<sub>2</sub>W<sub>14</sub>} units reported by Izarova and Kögerler<sup>32</sup> and by Yan and Su<sup>21</sup> or from the { $\alpha$ -P<sub>2</sub>W<sub>14</sub>O<sub>54</sub>}<sup>14-</sup> unit reported by Gouzerh et al. in 2005.<sup>34</sup> This { $\gamma$ -Se<sub>2</sub>W<sub>14</sub>O<sub>52</sub>} tetravacant Dawson structure is relatively rare and was, to our knowledge, only reported by Cronin and coworkers in 2014 as a building unit of compound [H<sub>12</sub>Pd<sub>10</sub>Se<sub>10</sub>W<sub>52</sub>O<sub>206</sub>]<sup>28-17</sup>. They are also related to the gamma isomer of the hexavacant {Se<sub>2</sub>W<sub>12</sub>} unit reported by Kalinina and Kortz<sup>16</sup> or by Long and Cronin<sup>33</sup> in cyclic systems [(Se<sub>2</sub>W<sub>12</sub>O<sub>46</sub>(WO(H<sub>2</sub>O))<sub>3</sub>)<sup>24-</sup> and [Se<sub>8</sub>W<sub>48</sub>O<sub>176</sub>]<sup>32-</sup> and also to the { $\gamma$ -Se<sub>2</sub>W<sub>13</sub>} pentavacant unit found in compound [Se<sub>4</sub>Pd<sub>4</sub>W<sub>28</sub>O<sub>108</sub>H<sub>12</sub>]<sup>12-32</sup>. Due to the lone pair of selenium, a tetravacant Dawson-type structure is obtained. As shown in Figure 2a, eight nucleophilic oxygen atoms are available and organized for coordinating four clusters [Mo<sub>2</sub>O<sub>2</sub>( $\mu$ -S)<sub>2</sub>(H<sub>2</sub>O)<sub>2</sub>]<sup>2+</sup> each, in two equatorial positions of the Mo(V) atoms (Figure 2b). Two dispositions of the [Mo<sub>2</sub>O<sub>2</sub>( $\mu$ -S)<sub>2</sub>(H<sub>2</sub>O)<sub>2</sub>]<sup>2+</sup> are possible, i.e. Mo=O short bonds or longer Mo-OH<sub>2</sub> bonds orientated towards the cavity. Therefore, one of the six {Mo<sub>2</sub>O<sub>2</sub>( $\mu$ -S)<sub>2</sub>(H<sub>2</sub>O)<sub>2</sub>]<sup>2+</sup> linkers has

water molecules oriented towards the inside of the cavity of the anion  $\{(\text{Se}_2\text{W}_{14}\text{O}_{52})_3(\text{Mo}_2\text{O}_2(\mu\text{-S})(\text{H}_2\text{O})_2)_6\}^{24-}$ , another one has outward-coordinated  $\text{H}_2\text{O}$  (Figure S4, SI), and the four remaining units show disorder between these two positions with a statistical distribution of water and oxo ligands pointing towards the cavity. This kind of disorder can be found in other  $[\text{Mo}_2\text{O}_2\text{S}_2]$ -containing POMs, such as  $[(\text{PW}_{11}\text{O}_{39})_2(\text{Mo}_4\text{S}_4\text{O}_4(\text{OH}_2)_2)]^{10-}$ ,<sup>26</sup> and  $[(\text{P}_2\text{W}_{17}\text{O}_{61})_2(\text{Mo}_4\text{S}_4\text{O}_4(\text{OH}_2)_2)]^{16-}$ .<sup>35</sup> Finally, the cavity of  $\{(\gamma\text{-Se}_2\text{W}_{14}\text{O}_{52})_3(\text{Mo}_2\text{O}_2(\mu\text{-S})(\text{H}_2\text{O})_2)_6\}^{24-}$  is occupied with two atoms with interatomic distance of 2.78 Å. They could be assigned as  $\text{Na}^+$  and  $\text{H}_2\text{O}$  with full occupancy distributed statistically over the two positions or to one  $\text{K}^+$  cation distributed over the two positions. This second hypothesis seems to be more realistic since M-O distances found in the 2.999-3.096 Å range are significantly longer than expected Na-O distances (from CCDC data bank, Na-O are mainly found in the 2.1-2.5 Å range) and much closer to the K-O distances reported in the CCDC data bank (usually K-O distances are mainly reported in the 2.5-3.0 Å range). Therefore, according to the elemental analysis evidencing the presence of potassium cations in the compound despite a recrystallization step in NaCl 0.1M solution, the presence of one potassium cation distributed between two positions must be considered (K1 with SOF = 0.7 and K2 with SOF = 0.3). Such a situation would lower the symmetry of **1** from  $D_{3h}$  to  $C_{3v}$  in the hypothesis that the exchange between the two positions is slow. The latter probably plays a role of template or stabilizing agent for such architecture. In other compounds associating  $\{\text{AsW}_9\}$  units and  $(\text{Mo}_2\text{O}_2\text{S}_2(\text{H}_2\text{O})_2)$  linkers, various supramolecular architectures were obtained by our group, strongly depending on the experimental conditions.<sup>11</sup> In particular triangular moieties  $\{(\text{AsW}_9)_3(\text{Mo}_2\text{O}_2\text{S}_2(\text{H}_2\text{O})_2)_3\}$  incorporating  $\text{Na}^+$ ,  $\text{K}^+$  or  $\text{H}_2\text{O}$  in the cavity were studied. Interestingly, we evidenced the stabilizing role of the  $\text{K}^+$  cation for such assemblies. When  $\text{K}^+$  is removed, the structure is irreversibly modified. A similar stabilizing role of  $\text{K}^+$  cation in  $\{(\gamma\text{-Se}_2\text{W}_{14}\text{O}_{52})_3(\text{Mo}_2\text{O}_2(\mu\text{-S})(\text{H}_2\text{O})_2)_6\}^{24-}$  is expected.

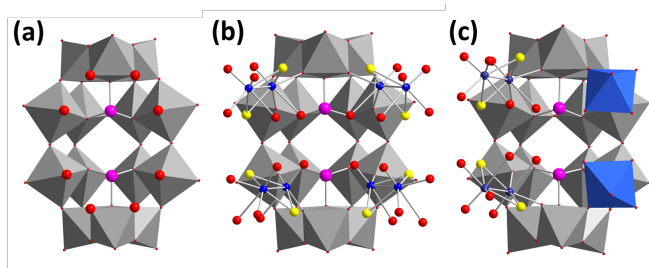


Figure 2. (a) Representation of the tetravacant  $\gamma\text{-Se}_2\text{W}_{14}$  unit found in anions **1** and **2**. The eight nucleophilic oxygen atoms are highlighted in red. (b) Picture of the connection of four  $[\text{Mo}_2\text{O}_2\text{S}_2(\text{H}_2\text{O})_2]^{2+}$  linkers to the eight available oxygen atoms of the  $\text{Se}_2\text{W}_{14}$  units found in **1**. (c) Picture of the connection of two  $[\text{Mo}_2\text{O}_2\text{S}_2(\text{H}_2\text{O})_2]^{2+}$  linkers and two  $\text{WO}_6$  octahedra (in fact  $\{\text{WO}_3(\text{H}_2\text{O})\}$ ) depicted in blue to the  $\gamma\text{-Se}_2\text{W}_{14}$  units found in compound **2**. The eight available oxygen atoms of the  $\text{Se}_2\text{W}_{14}$  units are coordinated in similar modes to those found in **1**.

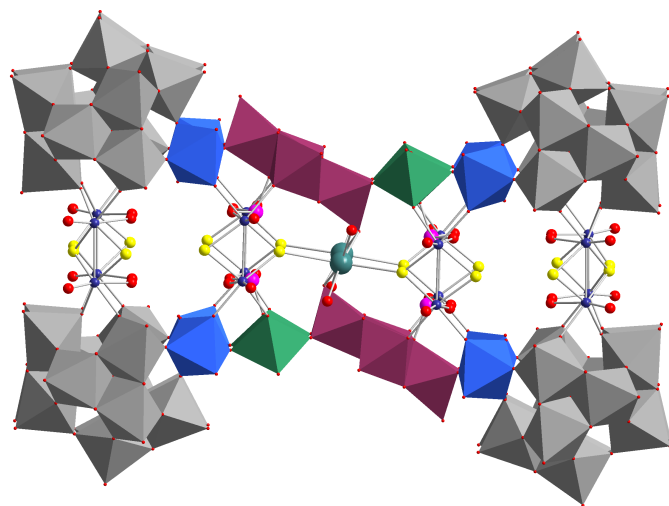


Figure 3. Molecular structure of polyanion **2**.  $\{\gamma\text{-Se}_2\text{W}_{14}\text{O}_{52}\}$  units are represented in grey polyhedra;  $[\text{Mo}_2\text{O}_2\text{S}_2(\text{H}_2\text{O})_2]^{2+}$  linkers are depicted in ball and stick (Mo in blue, S in yellow, O in red);  $\{\text{WO}_3(\text{H}_2\text{O})\}$  units are depicted as blue octahedra; isopolytungstates moieties  $\{\text{W}_2\text{O}_5\}$  and  $\{\text{W}_4\text{O}_{12}\}$  are given in red and green respectively; additional  $\text{SeO}_3^{2-}$  anions can be identified through the Se atoms depicted as pink spheres.

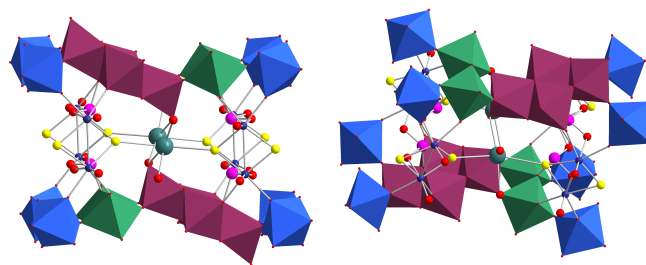


Figure 4. Highlights of the central part of the anion **2** showing the connections  $[\text{Mo}_2\text{O}_2\text{S}_2]^{2+}$  linkers (Mo in blue, S in yellow, O in red),  $\{\text{WO}_3(\text{H}_2\text{O})\}$  units (blue octahedra); isopolytungstates moieties  $\{\text{W}_2\text{O}_5\}$  and  $\{\text{W}_4\text{O}_{12}\}$  (red and green polyhedra respectively), the additional  $\text{SeO}_3^{2-}$  anions (Se as pink spheres) and the two central sodium cations (green spheres).

By mixing the same reactants in aqueous medium, the color becomes much darker when the pH is decreased below 2.5 and the synthetic solution kept in air at pH 2 gave single crystals of a compound of the formula  $\text{Na}_{35}\text{K}_3\text{H}_2[(\gamma\text{-Se}_2\text{W}_{14}\text{O}_{52})_4(\text{WO}_3(\text{H}_2\text{O}))_8(\text{W}_2\text{O}_5)_2(\text{W}_4\text{O}_{12})_2(\text{Mo}_2\text{O}_2(\mu\text{-S})(\text{H}_2\text{O})_2)_4(\text{Mo}_2\text{O}_2(\mu\text{-S})(\text{SeO}_3))_4]\cdot 120\text{H}_2\text{O}$ , abbreviated hereafter **Na-2**. At this pH, the formation of the  $[\text{Mo}_8\text{O}_8\text{S}_8(\text{OH})_8(\text{HWO}_5(\text{H}_2\text{O}))]^{3-}$  compound does not occur and the synthetic one pot procedure has been optimized by using stoichiometric amounts of each components. **Na-2** crystallizes in the triclinic P-1 space group. As depicted in Figure 3 and in Figure S5 (Supporting Information), the large anion  $[(\gamma\text{-Se}_2\text{W}_{14}\text{O}_{52})_4(\text{WO}_3(\text{H}_2\text{O}))_8(\text{W}_2\text{O}_5)_2(\text{W}_4\text{O}_{12})_2(\text{Mo}_2\text{O}_2(\mu\text{-S})(\text{H}_2\text{O})_2)_4(\text{Mo}_2\text{O}_2(\mu\text{-S})(\text{SeO}_3))_4]^{40-}$ , namely **2**, possesses nanometric dimensions  $3 \times 2.2$  nm. In contrast to the synthesis of **1**, the synthesis of **2** is performed at lower pH, which can significantly modify

the condensation processes of isopolytungstates. The anion **2** can be decomposed into 6 building blocks of different sizes: four tetravacant  $\{\gamma\text{-Se}_2\text{W}_{14}\text{O}_{52}\}$  units (in grey in Figure 3); eight monotungstate groups  $\{\text{WO}_3(\text{H}_2\text{O})\}$  (in blue), two dinuclear units  $\{\text{W}_2\text{O}_5\}$  (in green), two tetratungstate units  $\{\text{W}_4\text{O}_{12}\}$  (in purple), eight  $\{\text{Mo}_2\text{O}_2\text{S}_2\}$  clusters divided into two types (depicted in ball and stick representation), and four additional selenite anions  $\text{SeO}_3^{2-}$  (Se in pink sphere). The main part of the hybrid anion consists of four tetravacant  $\{\gamma\text{-Se}_2\text{W}_{14}\text{O}_{52}\}$  fragments on which are coordinated two outside  $\{\text{Mo}_2\text{O}_2(\mu_2\text{-S})_2(\text{H}_2\text{O})_2\}^{2+}$  clusters and two tungstate  $\{\text{WO}_3(\text{H}_2\text{O})\}$  units (see Figure 2c). The two  $\{\text{Mo}_2\text{O}_2(\mu_2\text{-S})_2(\text{H}_2\text{O})_2\}^{2+}$  are connected on their opposite equatorial positions with another  $\{\gamma\text{-Se}_2\text{W}_{14}\text{O}_{52}\}$  fragment to give a  $\{\gamma\text{-Se}_2\text{W}_{14}\text{O}_{52}\}_2(\text{Mo}_2\text{O}_2\text{S}_2(\text{H}_2\text{O})_2)_2$  moiety which can be seen as a fragment of the anion **1**. Furthermore, as observed in **1**, both outside  $\{\text{Mo}_2\text{O}_2(\mu_2\text{-S})_2(\text{H}_2\text{O})_2\}^{2+}$  clusters experience disorder over two close positions with 0.65/0.35 SOF values. This fact can be viewed as usual rotation of the  $\{\text{Mo}_2\text{O}_2(\mu_2\text{-S})_2(\text{H}_2\text{O})_2\}^{2+}$  units. Each  $\{\text{WO}_3(\text{H}_2\text{O})\}$  unit connected to the  $\{\gamma\text{-Se}_2\text{W}_{14}\text{O}_{52}\}$  POM bridges either a  $\{\text{W}_2\text{O}_5\}$  or a  $\{\text{W}_4\text{O}_{12}\}$  unit and the two latter are also connected together by sharing summits (see Figure S5, SI). Finally, the inner  $\{\text{Mo}_2\text{O}_2(\mu_2\text{-S})_2\}^{2+}$  units have two  $\text{SeO}_3^{2-}$  ligands coordinated into trans positions to the  $\text{Mo}=\text{O}$  units, which connect two  $\{\text{Mo}_2\text{O}_2(\mu_2\text{-S})_2\}^{2+}$  fragments together. Such coordination of  $\text{SeO}_3^{2-}$  is not surprising if we consider the family of cyclic compounds discovered by Miras and Cronin.<sup>36-37</sup> All the  $\text{Mo}=\text{O}$  bonds are directed outside the POM (Figures S6, SI). Moreover, these clusters are coordinated through oxygen atoms of  $\{\text{W}_2\text{O}_5\}$  groups in the cis-positions (one of oxygen atom of  $\text{SeO}_3^{2-}$  participates in the formation of  $\{\text{W}_2\text{O}_6\}$  moiety). Other cis-positions are occupied by oxygen atoms of the rhombohedral  $\{\text{W}_4\text{O}_{12}\}$  fragment (Figures S5-S6, SI). Four inner  $\{\text{Mo}_2\text{O}_2(\mu_2\text{-S})_2\}^{2+}$  units, two  $\{\text{W}_4\text{O}_{12}\}$  and two  $\{\text{W}_2\text{O}_5\}$  groups form the cavity in the central part of this hybrid polyoxometalate which is depicted in Figure 4. Finally, the cavity of **2** is partially filled by two sodium cations with SOF = 0.6 in interaction with two bridging sulfide of two  $\{\text{Mo}_2\text{O}_2(\mu_2\text{-S})_2\}^{2+}$  clusters (Na-S = 2.972 and 3.031 Å), two water molecules (Na-Ow = 2.267 and 2.432 Å), and two terminal oxo ligands of the  $\{\text{W}_4\text{O}_{12}\}$  units (Na-O = 2.491 and 2.495 Å) leading to distorted octahedra.

## Nuclear magnetic resonance spectroscopy

The two polyanions were tentatively characterized by  $^{77}\text{Se}$  and  $^{183}\text{W}$  NMR in  $\text{H}_2\text{O}\text{-D}_2\text{O}$  solution. Unfortunately, as shown in Figure S8 (SI), we were not able to confidently analyze the  $^{183}\text{W}$  spectra for these two compounds in aqueous medium. The spectrum of **2** was too poor and only some broad signals can be hardly seen. Usually giant POMs with high nuclearity exceeding 60 W atoms are difficult to measure by  $^{183}\text{W}$  NMR probably due to the combination of low symmetry of their structure and their slow tumbling motion causing dispersion and broadening of their signals. In the case of compound **1**, a complex spectrum is obtained containing at least twenty-six resonances. In line with this,  $^{77}\text{Se}$  NMR (Figure S9) also showed many resonances instead of one or two signals expected for the idealized high symmetrical structure  $D_{3h}$  or  $C_{3v}$  of **1**, and broad signals for **2** ranging from 1260 to 1360 ppm. Similar difficulties were also reported by Kortz and Kalinina for cyclic compound resulting from the connection of three  $\{\text{Se}_2\text{W}_{12}\}$  fragments to  $\{\text{WO}(\text{H}_2\text{O})\}^{4+}$  groups.<sup>16</sup> They showed evolution of the  $^{77}\text{Se}$  spectrum with time leading to a myriad of signals within the range 1240-1350 ppm. They concluded the sample is unstable in aqueous solution and the solid-state  $^{77}\text{Se}$  MAS spectrum exhibited a broad signal covering the 1287-1293 ppm range. In Figure 5, the  $^{77}\text{Se}$  MAS spectra of samples **1** and **2** show similar resonances at ca. 1305-1308 and 1294-

1301 ppm respectively, that should account for typical selenium sites in selenotungstate derivatives. Coming back to solution studies, if we consider that single crystals of **1** and **2** are obtained with correct yields in 10 days, the decomposition of our product cannot explain these results. All these observations would be better explained in terms of local disorders of the components of **1** and **2**, which produces mixture of isomers with lower symmetries. As example, for compound **1**, the disorders of each of the six  $(\text{Mo}_2\text{O}_2\text{S}_2(\text{H}_2\text{O})_2)^{2+}$  linkers over two possible positions lead at least to 14 isomers. Additionally, if we consider that the exchange of the potassium cation over its two positions is slow, this number increases to 18 isomers displaying symmetries ranging from  $C_{3v}$  to  $C_1$ , which translates by 2 to 6 NMR lines for  $^{77}\text{Se}$  and by 4 to 42 lines for  $^{183}\text{W}$  NMR spectra. Besides, due to the high lability of the  $(\text{Mo}_2\text{O}_2\text{S}_2(\text{H}_2\text{O})_2)^{2+}$  linkers,<sup>9,10</sup> we also cannot exclude some decoordination/coordination processes of the latter leading to equilibria with smaller species of low symmetries as observed by ESI-MS. This second phenomenon should occur more likely for the bigger compound **2**.

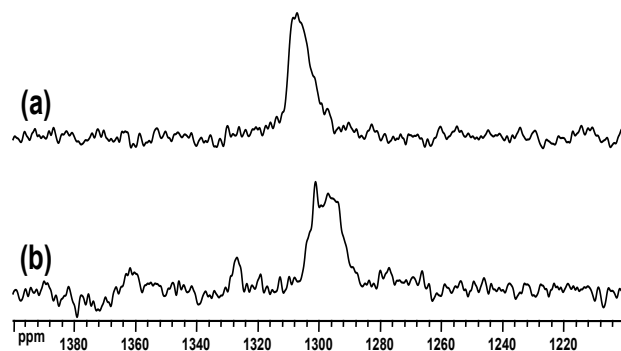


Figure 5. MAS  $^{77}\text{Se}$  NMR spectra of (a) Na-1 and (b) Na-2.

## Electrospray Ionization Mass Spectrometry

ESI-MS characterization of such high nuclearity POMs is not trivial in aqueous medium because of their high molecular weights, high charge states and their limited chemical stability. Besides, ionization occurs via multiple associations with alkali cations and protons along with solvent water molecules. Hence, very broad peaks are observed in their corresponding ESI mass spectra, which ultimately preclude accurate determination of the composition of the POMs. Cronin's group pioneered the use of ESI-MS for the identification of gigantic polyanions in solution on the basis of the observation of polyanions with differing numbers of cations and water molecules existing either as monomers or oligomers of the related parent polyanion.<sup>19, 38-39</sup> Molecular weights can be estimated by ESI-MS via deconvolution of multiply charged states of intact polyanion taking into consideration the spacing between the series of broad peaks in the ESI mass spectra. In this context, the ESI mass spectra of  $10^{-4}$  M aqueous solutions of compounds **Na-1** and **Na-2** were investigated. As shown in Figure 6, the ESI-MS spectrum of **Na-1** displays three broad peaks centered at  $m/z$  1820, 2124 and 2600 encompassing 7- to 5-charge states. The ESI mass spectrum of compound **Na-2** shows five broad peaks centered at  $m/z$  2066, 2275, 2532, 2858 and 3287 encompassing from 11- to 7- charge states, along with two broad peaks at  $m/z$  2036 and 2078 that are probably due to partially dismantled POM. Additionally, dimers derived from **2** were also observed in the gas phase at  $m/z$  3545 and 3850 as typically found in closely related gigantic POMs.<sup>19,38-39</sup> In general, accurate peak assignments are not possible because of the inherent broadness of the peaks due to interaction with cations ( $\text{H}^+$ ,  $\text{Na}^+$  or  $\text{K}^+$ )

and partial removal of water molecules or hydration; however, from the  $m/z$  values and the charge state determination, it is evidenced that the integrity of the two large polyanions  $[(W_{14}Se_2O_{52})_3(Mo_2O_2(S)_2(H_2O)_2)_6]^{24-}$  (**1**) and  $[(Se_2W_{14}O_{52})_4(WO_3(H_2O))_8(W_2O_5)_2(W_4O_{13})_2(Mo_2O_2S_2(H_2O)_2)_4(Mo_2O_2S_2(SeO_3))_4]^{40-}$  (**2**) is preserved in solution during the time needed for ES-MS experiment. Table S1 in supporting information gives some possible assignments among many possibilities. Besides, either for **Na-1** or **Na-2**, triply and doubly-charged species at  $m/z$  values below 1700 were also observed as broad peaks (see Figure S10 and S11, SI). It is clear that  $m/z$  values in the 1250-1450 range with 3- charges must be reasonably due to the presence of the fragments  $[(Se_2W_{14}O_{52})(Mo_2O_2S_2)_n]$  with  $n = 1-3$ , associated with  $H^+$ ,  $Na^+$  and water molecules. The relative intensity of these species with respect to **1** (or **2**) remained largely unchanged for 30 minutes, thus suggesting that, rather than decomposition of **1** (or **2**), they are formed under the ESI conditions. Other building blocks such as the  $[(Se_2W_{14}O_{52})_2(Mo_2O_2S_2)_n]$  are not observed at all.

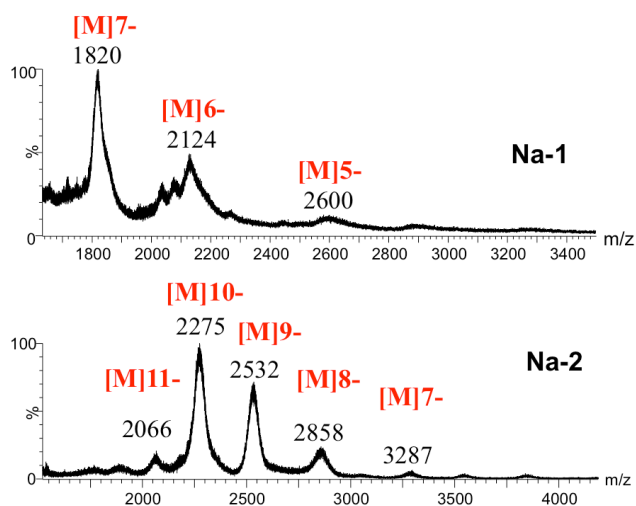


Figure 6. Negative ESI-MS spectra of aqueous solutions ( $10^{-4}$  M) of **Na-1** and **Na-2** at a cone voltage of  $U_c = 10$  V.

## Conclusion

Among the experimental factors, the control of pH is a key parameter in the formation of POMs, and thus the pH dependent synthetic approach constitutes an important research objective for the rational design of giant POM assemblies. Herein, we exemplify the feasibility of one-pot procedures to selectively isolate two original giant heteropolyoxotungstates containing a rare  $\{\gamma\text{-}Se_2W_{14}\}$  tetravacant selenotungstate building block. The synthetic entry proceeds under soft conditions at room temperature and atmospheric pressure by mixing some sodium tungstate, selenium dioxide, and an  $[Mo_2O_2S_2(H_2O)_6]^{2+}$  precursor in water, at two different pH values:  $[(\gamma\text{-}Se_2W_{14}O_{52})_3(Mo_2O_2(\mu\text{-}S)_2(H_2O)_2)_6]^{24-}$  (**1**) isolated at pH 3.5 and  $[(\gamma\text{-}Se_2W_{14}O_{52})_4(WO_3(H_2O))_8(W_2O_5)_2(W_4O_{13})_2(Mo_2O_2(\mu\text{-}S)_2(H_2O)_2)_4(Mo_2O_2(\mu\text{-}S)_2(SeO_3))_4]^{40-}$  (**2**) at pH 2. The two compounds were characterized in the solid state by single crystal X-Ray diffraction, EDX, elemental analysis, TGA, FT-IR, and  $^{77}Se$

solid state NMR. Solution state NMR studies revealed however complex spectra, probably due to the formation of number of isomers and to some equilibria with some smaller species evidenced by ESI-MS. We nevertheless succeeded to evidence the presence of the intact anions **1** and **2** in water at  $10^{-4}$  M by ESI-MS that were accompanied by peaks correlated to smaller  $[(Se_2W_{14}O_{52})(Mo_2O_2S_2)_n]$  with  $n = 1-3$  fragments due to fragmentation upon ESI conditions. Finally, these results probably pave the way towards a fascinating family of compounds in the ternary system  $WO_4^{2-}$ ,  $SeO_3^{2-}$ , and  $[Mo_2O_2S_2(H_2O)_6]^{2+}$  by exploring the effect of the pH and the stoichiometric ratio.

## ASSOCIATED CONTENT

### Supporting Information

FT-IR Spectra of **Na-1** and **Na-2** (Figures S1-S2); additional structural representations of compounds **1** and **2** (Figure S3-S7);  $^{183}W$  and  $^{77}Se$  NMR spectra recorded for **Na-1** and **Na-2** (Figures S8 and S9) and additional ESI-MS spectra of **Na-1** and **Na-2** (Figures S10-S11).

## AUTHOR INFORMATION

### Corresponding Authors

Dr Sébastien Floquet : [sebastien.floquet@uvsq.fr](mailto:sebastien.floquet@uvsq.fr)

Dr Pavel A. Abramov : [abramov@niic.nsc.ru](mailto:abramov@niic.nsc.ru)

### Author Contributions

The manuscript was written through contributions of all authors. All authors have given approval to the final version of the manuscript.

### Notes

The authors declare no competing financial interests.

## ACKNOWLEDGMENT

This work was supported LIA FRANCE-RUSSIA No. 1144 CLUSPOM and COST STSM program (COST-STSM-ECOST-STSM-CM1203-101015-062506). The “Institut Universitaire de France” (IUF), the CNRS and University of Versailles are also acknowledged for the financial support. SCIC of the University Jaume I is acknowledged for providing ESI-MS facilities. Dr Nathalie Leclerc is also gratefully acknowledged for her help for TGA and EDX measurements.

## REFERENCES

- Carraro, M.; Fiorani, G.; Mognon, L.; Caneva, F.; Gardan, M.; Maccato, C.; Bonchio, M., Hybrid Polyoxotungstates as Functional Comonomers in New Cross-Linked Catalytic Polymers for Sustainable Oxidation with Hydrogen Peroxide. *Chem.-Eur. J.* **2012**, *18* (41), 13195-13202.
- Nohra, B.; El Moll, H.; Albelo, L. M. R.; Mialane, P.; Marrot, J.; Mellot-Draznieks, C.; O'Keeffe, M.; Biboum, R. N.; Lemaire, J.; Keita, B.; Nadjo, L.; Dolbecq, A., Polyoxometalate-Based Metal Organic Frameworks (POMOFs): Structural Trends, Energetics, and High Electrocatalytic Efficiency for Hydrogen Evolution Reaction. *J. Am. Chem. Soc.* **2011**, *133* (34), 13363-13374.
- Barsukova-Stuckart, M.; Piedra-Garza, L. F.; Gautam, B.; Alfaro-Espinoza, G.; Izarova, N. V.; Banerjee, A.; Bassil, B. S.; Ullrich, M. S.; Breunig, H. J.; Silvestru, C.; Korts, U., Synthesis and Biological Activity of Organoantimony(III)-Containing Heteropolytungstates. *Inorg. Chem.* **2012**, *51* (21), 12015-12022.
- Charron, G.; Giusti, A.; Mazerat, S.; Mialane, P.; Gloter, A.; Miserque, F.; Keita, B.; Nadjo, L.; Filoramo, A.; Riviere, E.; Wernsdorfer, W.; Huc, V.; Bourgoin, J. P.; Mallah, T., Assembly of a magnetic polyoxometalate on SWNTs. *Nanoscale* **2010**, *2* (1), 139-144.

5. Symes, M. D.; Kitson, P. J.; Yan, J.; Richmond, C. J.; Cooper, G. J. T.; Bowman, R. W.; Vilbrandt, T.; Cronin, L., Integrated 3D-printed reactionware for chemical synthesis and analysis. *Nat. Chem.* **2012**, *4* (5), 349-354.
6. Long, D. L.; Tsunashima, R.; Cronin, L., Polyoxometalates: Building Blocks for Functional Nanoscale Systems. *Angew. Chem.-Int. Edit.* **2010**, *49* (10), 1736-1758.
7. Müller, A.; Gouzerh, P., From linking of metal-oxide building blocks in a dynamic library to giant clusters with unique properties and towards adaptive chemistry. *Chem. Soc. Rev.* **2012**, *41* (22), 7431-7463.
8. Müller, A.; Gouzerh, P., Capsules with Highly Active Pores and Interiors: Versatile Platforms at the Nanoscale. *Chem.-Eur. J.* **2014**, *20* (17), 4862-4873.
9. Lemonnier, J. F.; Duval, S.; Floquet, S.; Cadot, E., A Decade of Oxothiomolybdenum Wheels: Synthesis, Behavior in Solution, and Electrocatalytic Properties. *Isr. J. Chem.* **2011**, *51* (2), 290-302.
10. Cadot, E.; Sokolov, M. N.; Fedin, V. P.; Simonnet-Jégat, C.; Floquet, S.; Sécheresse, F., A building block strategy to access sulfur-functionalized polyoxometalate based systems using  $\{\text{Mo}_2\text{S}_2\text{O}_2\}$  and  $\{\text{Mo}_3\text{S}_4\}$  as constitutional units, linkers or templates. *Chem. Soc. Rev.* **2012**, *41* (22), 7335-7353.
11. Marrot, J.; Pilette, M. A.; Haouas, M.; Floquet, S.; Taulelle, F.; Lopez, X.; Poblet, J. M.; Cadot, E., Polyoxometalates Paneling through  $\{\text{Mo}_2\text{O}_2\text{S}_2\}$  Coordination: Cation-Directed Conformations and Chemistry of a Supramolecular Hexameric Scaffold. *J. Am. Chem. Soc.* **2012**, *134* (3), 1724-1737.
12. Korenev, V. S.; Boulay, A. G.; Dolbecq, A.; Sokolov, M. N.; Hijazi, A.; Floquet, S.; Fedin, V. P.; Cadot, E., A New Oxomolybdate Component Extracted from the "Virtual Dynamic Library" Yielding the Macrocyclic Anion  $[(\text{Mo}_8\text{O}_{28})_4(\text{Mo}_2\text{O}_2\text{S}_2)_4]^{24-}$ . *Inorg. Chem.* **2010**, *49* (21), 9740-9742.
13. Korenev, V. S.; Boulay, A. G.; Haouas, M.; Bannani, F.; Fedin, V. P.; Sokolov, M. N.; Terazzi, E.; Garai, S.; Müller, A.; Taulelle, F.; Marrot, J.; Leclerc, N.; Floquet, S.; Cadot, E., Tracking "Apolar"  $\text{NMe}_4^+$  Ions within Two Polyoxothiomolybdates that Have the Same Pores: Smaller Clathrate and Larger Highly Porous Clusters in Action. *Chem.-Eur. J.* **2014**, *20* (11), 3097-3105.
14. Bannani, F.; Floquet, S.; Leclerc-Laronze, N.; Haouas, M.; Taulelle, F.; Marrot, J.; Kögerler, P.; Cadot, E., Cubic Box versus Spheroidal Capsule Built from Defect and Intact Pentagonal Units. *J. Am. Chem. Soc.* **2012**, *134* (47), 19342-19345.
15. Wang, L. J.; Li, W. J.; Wu, L. Z.; Dong, X. B.; Hu, H. M.; Xue, G. L., A new polyanion with Dawson-like constitution:  $\text{H}_2\text{SeW}_{18}\text{O}_{60}^{6-}$ . *Inorg. Chem. Commun.* **2013**, *35*, 122-125.
16. Kalinina, I. V.; Peresyphkina, E. V.; Izarova, N. V.; Nkala, F. M.; Kortz, U.; Kompankov, N. B.; Moroz, N. K.; Sokolov, M. N., Cyclic Tungstoselenites Based on  $\{\text{Se}_2\text{W}_{12}\}$  Units. *Inorg. Chem.* **2014**, *53* (4), 2076-2082.
17. Cameron, J. M.; Gao, J.; Long, D.-L.; Cronin, L., Self-assembly and structural transformations of high-nuclearity palladium-rich polyoxometalates. *Inorg. Chem. Front.* **2014**, *1* (2), 178-185.
18. Yan, J.; Long, D. L.; Cronin, L., Development of a Building Block Strategy To Access Gigantic Nanoscale Heteropolyoxotungstates by Using  $\text{SeO}_3^{2-}$  as a Template Linker. *Angew. Chem.-Int. Edit.* **2010**, *49* (24), 4117-4120.
19. Gao, J.; Yan, J.; Beeg, S.; Long, D. L.; Cronin, L., One-Pot versus Sequential Reactions in the Self-Assembly of Gigantic Nanoscale Polyoxotungstates. *J. Am. Chem. Soc.* **2013**, *135* (5), 1796-1805.
20. Chen, W. C.; Li, H. L.; Wang, X. L.; Shao, K. Z.; Su, Z. M.; Wang, E. B., Assembly of Cerium(III)-Stabilized Polyoxotungstate Nanoclusters with  $\text{SeO}_3^{2-}/\text{TeO}_3^{2-}$  Templates: From Single Polyoxoanions to Inorganic Hollow Spheres in Dilute Solution. *Chem.-Eur. J.* **2013**, *19* (33), 11007-11015.
21. Chen, W. C.; Yan, L. K.; Wu, C. X.; Wang, X. L.; Shao, K. Z.; Su, Z. M.; Wang, E. B., Assembly of Keggin/Dawson-type Polyoxotungstate Clusters with Different Metal Units and  $\text{SeO}_3^{2-}$  Heteroanion Templates. *Cryst. Growth Des.* **2014**, *14* (10), 5099-5110.
22. Milne, J., Chemical-shift references for Se-77 NMR spectroscopy - selenous acid. *Magn. Reson. Chem.* **1993**, *31* (7), 652-655.
23. Sheldrick, G. M. *SADABS program for scaling and correction of area detector data*, SADABS program for scaling and correction of area detector data, University of Göttingen, Germany., 1997.
24. Sheldrick, G. M., Crystal structure refinement with SHELXL. *Acta Cryst.* **2015**, *C71*, 3-8.
25. Hübschle, C. B.; Sheldrick, G. M.; Dittrich, B., ShelXle: a Qt graphical user interface for SHELXL. *J. Appl. Cryst.* **2011**, *44*, 1281-1284.
26. Marrot, J.; Pilette, M. A.; Sécheresse, F.; Cadot, E., A monovacant heteropolytungstate thioderivative: Synthesis and characterization of  $(\text{PW}_{11}\text{O}_{39})_2(\text{H}_4\text{Mo}_4\text{S}_4\text{O}_6)^{10-}$  and related isomers. *Inorg. Chem.* **2003**, *42* (11), 3609-3615.
27. Cadot, E.; Salignac, B.; Marrot, J.; Dolbecq, A.; Sécheresse, F.,  $\text{Mo}_{10}\text{S}_{10}\text{O}_{10}(\text{OH})_{10}(\text{H}_2\text{O})_5$ : a novel decameric molecular ring showing supramolecular properties. *Chem. Commun.* **2000**, (4), 261-262.
28. Korenev, V. S.; Floquet, S.; Marrot, J.; Haouas, M.; Mbomekalle, I. M.; Taulelle, F.; Sokolov, M. N.; Fedin, V. P.; Cadot, E., Oxothiomolybdenum Derivatives of the Superlacunary Crown Heteropolyanion  $\{\text{P}_8\text{W}_{48}\}$ : Structure of  $\text{K}_4\{\text{Mo}_4\text{O}_4\text{S}_4(\text{H}_2\text{O})_3(\text{OH})_2\}_2(\text{WO}_2)(\text{P}_8\text{W}_{48}\text{O}_{184})^{30-}$  and Studies in Solution. *Inorg. Chem.* **2012**, *51* (4), 2349-2358.
29. Korenev, V. S.; Abramov, P. A.; Vicent, C.; Mainichev, D. A.; Floquet, S.; Cadot, E.; Sokolov, M. N.; Fedin, V. P., Trapping  $\{\text{BW}_{12}\}_2$  tungstoborate: synthesis and crystal structure of hybrid  $\{\text{H}_2\text{BW}_{12}\text{O}_{42}\}_2\{\text{Mo}_6\text{O}_6\text{S}_6(\text{OH})_4(\text{H}_2\text{O})_2\}^{14-}$  anion. *Dalton Trans.* **2012**, *41* (48), 14484-14486.
30. Cadot, E.; Sécheresse, F., Cyclic molecular materials based on  $\text{M}_2\text{O}_2\text{S}_2^{2-}$  cores (M = Mo or W). *Chem. Commun.* **2002**, (19), 2189-2197.
31. Dolbecq, A.; du Peloux, C.; Auberty, A. L.; Mason, S. A.; Barboux, P.; Marrot, J.; Cadot, E.; Sécheresse, F., Synthesis, X-ray and neutron diffraction characterization, and ionic conduction properties of a new oxothiomolybdate  $\text{Li}_3\text{Mo}_8\text{S}_8\text{O}_8(\text{OH})_8\{\text{HWO}_3(\text{H}_2\text{O})\} \cdot 18\text{H}_2\text{O}$ . *Chem.-Eur. J.* **2002**, *8* (2), 350-356.
32. Izarova, N. V.; Santiago-Schubel, B.; Willbold, S.; Hess, V.; Kögerler, P., Classical/Non-classical Polyoxometalate Hybrids. *Chem.-Eur. J.* **2016**, *22* (45), 16052-16056.
33. Cameron, J. M.; Gao, J.; Vila-Nadal, L.; Long, D. L.; Cronin, L., Formation, self-assembly and transformation of a transient selenotungstate building block into clusters, chains and macrocycles. *Chem. Commun.* **2014**, *50* (17), 2155-2157.
34. Godin, B.; Vaissermann, J.; Herson, P.; Ruhlmann, L.; Verdager, M.; Gouzerh, P., Coordination chemistry of the hexavacant tungstophosphate  $\text{H}_2\text{P}_2\text{W}_{12}\text{O}_{48}^{12-}$ : synthesis and characterization of iron(III) complexes derived from the unprecedented  $\{\text{P}_2\text{W}_{14}\text{O}_{54}\}$  fragment. *Chem. Commun.* **2005**, (45), 5624-5626.
35. Pilette, M. A.; Floquet, S.; Marrot, J.; Cadot, E., Synthesis, Structure, and Behavior in Solution of the Dawson Thio Derivative  $(\text{P}_2\text{W}_{17}\text{O}_{61})_2(\text{H}_4\text{Mo}_4\text{S}_4\text{O}_6)^{16-}$ . *Eur. J. Inorg. Chem.* **2011**, (23), 3523-3528.
36. Zang, H. Y.; Chen, J. J.; Long, D. L.; Cronin, L.; Miras, H. N., Assembly of inorganic  $\text{Mo}_2\text{O}_2\text{S}_2^{2+}$  panels connected by selenite anions to nanoscale chalcogenide-polyoxometalate clusters. *Chem. Sci.* **2016**, *7* (6), 3798-3804.
37. Zang, H. Y.; Chen, J. J.; Long, D. L.; Cronin, L.; Miras, H. N., Assembly of Thiometalate-Based  $\{\text{Mo}-16\}$  and  $\{\text{Mo}-36\}$  Composite Clusters Combining  $\text{Mo}_2\text{O}_2\text{S}_2^{2+}$  Cations and Selenite Anions. *Adv. Mater.* **2013**, *25* (43), 6245-6249.
38. Yan, J.; Gao, J.; Long, D. L.; Miras, H. N.; Cronin, L., Self-Assembly of a Nanosized, Saddle-Shaped, Solution-Stable Polyoxometalate Anion Built from Pentagonal Building Blocks:  $\text{H}_{34}\text{W}_{119}\text{Se}_8\text{Fe}_2\text{O}_{420}^{54-}$ . *J. Am. Chem. Soc.* **2010**, *132* (33), 11410-11411.
39. Gao, J.; Yan, J.; Beeg, S.; Long, D. L.; Cronin, L., Assembly of Molecular "Layered" Heteropolyoxometalate Architectures. *Angew. Chem.-Int. Edit.* **2012**, *51* (14), 3373-3376.

Self-assembly reactions between  $\text{Na}_2\text{WO}_4$ ,  $\text{SeO}_3^{2-}$  and  $[\text{Mo}_2\text{O}_2(\mu\text{-S})_2(\text{H}_2\text{O})_6]^{2+}$  in water give selectively two new large polyoxometalate complexes at  $\text{pH} = 2$  and  $\text{pH} = 3.5$ , namely  $[(\text{Se}_2\text{W}_{14}\text{O}_{52})_4(\text{WO}_3(\text{H}_2\text{O}))_8(\text{W}_2\text{O}_5)_2(\text{W}_4\text{O}_{12})_2(\text{Mo}_2\text{O}_2(\mu\text{-S})_2(\text{H}_2\text{O})_2)_4(\text{Mo}_2\text{O}_2(\mu\text{-S})_2(\text{SeO}_3))_4]^{36-}$  and  $[(\text{W}_{14}\text{Se}_2\text{O}_{52})_3(\text{Mo}_2\text{O}_2(\mu\text{-S})_2(\text{H}_2\text{O})_2)_6]^{24-}$ , respectively for which the building units were compared and discussed.

